Published in final edited form as:
J Neurosci. 2011 October 5; 31(40): 14204–14217. doi:10.1523/JNEUROSCI.3285-11.2011.

Cortical Projections of Functionally-Identified Thalamic Trigeminovascular neurons: Implications to Migraine Headache and Its Associated Symptoms

Rodrigo Noseda[1], **Moshe Jakubowski**[1], **Vanessa Kainz**[1], **David Borsook**[2], and **Rami Burstein**[1]

[1]Department of Anesthesia and Critical Care, Beth Israel Deaconess Medical Center, Harvard Medical School, Boston, MA 02215

[2]P.A.I.N. Group, Brain Imaging Center, Department of Psychiatry, Harvard Medical School, Belmont, MA

Abstract

This study identifies massive axonal arbors of trigeminovascular (dura-sensitive) thalamic neurons in multiple cortical areas and proposes a novel framework for conceptualizing migraine headache and its associated symptoms. Individual dura-sensitive neurons identified and characterized electrophysiologically in first-order and higher-order relay thalamic nuclei were juxtacellularly filled with an anterograde tracer that labeled their cell bodies and processes. First-order neurons located in the ventral posteromedial (VPM) nucleus projected mainly to trigeminal areas of primary (S1) as well as secondary (S2) somatosensory and insular cortices. Higher-order neurons located in the posterior (Po), lateral posterior (LP) and lateral dorsal (LD) nuclei projected to trigeminal and extratrigeminal areas of S1 and S2, as well as parietal association, retrosplenial, auditory, ectorhinal, motor and visual cortices. Axonal arbors spread at various densities across most layers of the different cortical areas. Such parallel network of thalamocortical projections may play different roles in the transmission of nociceptive signals from the meninges to the cortex. The findings that individual dura-sensitive Po neurons project to many functionally-distinct and anatomically-remote cortical areas extend current thinking on projection patterns of high-order thalamic neurons and position them to relay nociceptive information directly, rather than indirectly from one cortical area to another. Such extensive input to diverse cortical areas that are involved in regulation of affect, motor function, visual and auditory perception, spatial orientation, memory retrieval, and olfaction may explain some of the common disturbances in neurological functions during migraine.

Keywords

thalamocortical; pain; nociception; dura; insula; somatosensory; cortex

Introduction

The headache phase of a migraine attack is thought to be mediated by the trigeminovascular pathway. The pathway's primary afferents reside in the trigeminal ganglion, and their axons split into a peripheral branch innervating blood vessels in the cerebral dura and pia maters,

Correspondence – Rami Burstein, CLS-649, 3 Blackfan Circle Boston, MA 02215; Tel. (617) 735 2832; Fax (617) 735 2833; rburstei@bidmc.harvard.edu.

Authors have no conflict of interest to declare

and a central branch projecting to the spinal trigeminal nucleus (SpV). Cell bodies of second-order trigeminovascular neurons are found mainly in laminae I and V of the dorsal horn of the medulla and upper cervical (C1–2) spinal segments (Strassman et al., 1994). Cell bodies of third-order trigeminovascular neurons are found mainly in the posterior (Po) and ventral posteromedial (VPM) thalamic nuclei.

Electrophysiological and anatomical studies have characterized the physiologic response properties of neurons along the trigeminovascular pathway. The primary afferents are activated by mechanical and chemical stimuli emanating from the dura (Mayberg et al., 1981; Mayberg et al., 1984; Strassman et al., 1996; Levy and Strassman, 2002). Trigeminovascular SpV neurons process nociceptive signals from the dura together with various sensory signals they receive from the cornea, facial skin and cephalic and neck muscles (Davis and Dostrovsky, 1988a; Kaube et al., 1992; Strassman et al., 1994; Angus-Leppan et al., 1997; Ebersberger et al., 1997; Burstein et al., 1998; Yamamura et al., 1999). Trigeminovascular thalamic neurons receive and process nociceptive signals from the dura together with various sensory signals from all somatic dermatomes (Davis and Dostrovsky, 1988b; Zagami and Lambert, 1990, 1991; Angus-Leppan et al., 1995; Shields and Goadsby, 2005; Burstein et al., 2010).

Anatomical mapping of axonal projections and termination sites of peripheral and central trigeminovascular neurons remains largely scarce due to technical limitations. Neuronal tract tracing from the meninges was found to label primary-afferent soma in the trigeminal ganglion and their axonal processes in laminae I–IV of the upper cervical and medullary dorsal horn (Liu et al., 2004, 2008). Axonal projections of individual second-order dura-sensitive neurons were traced electrophysiologically from laminae I and V of SpV to the midbrain, where they bifurcated into one branch that projected to the Po, VPM, and parafascicular thalamic nuclei, and a second branch that projected to the anterior, lateral, perifornical and posterior hypothalamic nuclei, and lateral preoptic area (Burstein et al., 1998).

The axonal projections and termination fields of trigeminovascular thalamic neurons remains largely unexplored. In this study, we used a technique that combines single-unit recording with subsequent iontophoretic administration of an anterograde tracer into targeted trigeminovascular thalamic neurons, thus labeling individual cell bodies and their processes with exquisite details (Gauriau and Bernard, 2004). Using this approach, we have successfully mapped the axonal trajectory and cortical terminations of three thalamic neurons that were characterized as receiving nociceptive input from the dura and photic signals from the retina (Noseda et al., 2010). The aim of the current study was to map and compare the cortical projections of trigeminovascular neurons located in first-order and higher-order relay thalamic nuclei, which are thought to play differential roles in thalamocorticothalmic processing of sensory information (Sherman, 2005; Jones, 2009).

Materials and Methods

Animals and surgical procedures

Experiments were approved by the Beth Israel Deaconess Medical Center and Harvard Medical School standing committees on animal care, and conducted in accordance with the U.S. National Institutes of Health Guide for the Care and Use of Laboratory Animals. Male Sprague-Dawley rats (250–350 g) were initially anesthetized with methohexital sodium (45 mg/kg i.p.) for endotracheal intubation and cannulation of the right femoral vein. Each rat was then mounted on a stereotaxic frame and switched to inhalation anesthesia – a mixture of isoflurane and pure oxygen delivered at a rate of 100 ml/min. Craniotomies (see below) were performed using 2.5% isoflurane, while the subsequent experimental procedure was

carried out under 1–1.2% isoflurane. End-tidal C O_2, blood oxygen saturation, as well as breathing and heart rates, were monitored and kept within physiological values throughout the experiment. Core body temperature was maintained at 37°C using a heating blanket. To immobilize the rats during the experiment, a mixture of the muscle relaxants vecuronium and pancuronium (each 1 mg/ml in lactated Ringer's solution) was infused continuously via the intravenous cannula at a rate of 0.3 mg/kg/hr.

Two craniotomies were performed. A 4×4-mm craniotomy was made at the lambdoid suture on the left side of the skull to allow placement of a stimulating electrode on the dura overlying the transverse sinus. A 2×2-mm craniotomy was made on the right side of the skull (2.5 mm behind the coronal suture; 2.5 mm lateral to the midline) in order to access the thalamus with a micropipette that was used for single-unit recording and juxtacellular administration of an anterograde tracer into the target cell. The exposed dura was kept moist using a modified synthetic interstitial fluid (SIF; 135 mM NaCl, 5 mM KCl, 1 mM $MgCl_2$, 5 mM $CaCl_2$, 10 mM glucose and 10 mM Hepes, pH 7.2).

Single-unit recordings

A glass micropipette (20–30 MΩ impedance) was lowered into the right posterior thalamus in search of single-unit discharges invoked by electrical pulses (0.8 ms, 0.5–3.0 mA, 1 Hz) at the exposed contralateral dura. A neurons was identified as dura-sensitive if it exhibited discrete firing bouts in response to such electrical pulses, as well as mechanical (calibrated von-Frey monofilament) and chemical (1 M KCl) stimulation of the dura (Fig. 1*A*). A neuron that failed to respond to electrical, mechanical *and* chemical stimulation of any part of the exposed area of the dura was referred to as dura-insensitive. Whether or not such neurons were actually dura-insensitive could not be determined with certainty because it was technically impossible to test them for stimulation of the entire area of the cerebral dura. All neurons were further classified as nociceptive or non-nociceptive based on their somatosensitivity to innocuous (brush) and noxious (pinch) mechanical stimulation of cephalic and extracephalic skin (Fig. 1*B*, *C*). Real-time waveform discriminator was used to create and store a template for the action potential evoked in the neuron under study by electrical pulses on the dura; spikes of activity matching the template waveform were acquired and analyzed online and offline using Spike 2 software (CED, Cambridge, UK).

Juxtacellular iontophoresis

Once characterized electrophysiologically, each neuron was infiltrated with the anterograde tracer which was delivered iontophoretically from the recording micropipette as described before (Pinault, 1996). The recording micropipette was preloaded with 3% tetramethylrhodamine (TMR) dextran (3,000 MW, anionic, lysine fixable; D-3308, Invitrogen), and the tracer was administered into the target cell body using a computer-controlled microelectrode amplifier (Axoclamp 900A, Molecular Devices). Uptake of the tracer by the cell body was achieved by inducing bouts of neuronal firing in response to positive current pulses (1–10 nA) which were delivered repetitively (200 ms on/of intervals) over a period of 10–60 min (Pinault, 1996; Fig. 2B). At the end of the injection, infusion of muscle relaxants was discontinued, wounds were stitched and disinfected, the cannula was removed from the femoral vein, isoflurane concentration was reduced gradually, the endotracheal tube was removed, and the rat was allowed to resume spontaneous breathing under >95% oxygen saturation.

Tissue processing

After a survival period of 3 or 4 days, each rat was injected with an overdose of pentobarbital sodium (100 mg/kg i.p.) and received intracardiac perfusion of 200 ml heparinized saline, followed by 500 ml of a fixative solution consisting of 4%

paraformaldehyde, 0.05% picric acid, 0.1 M phosphate buffered saline (PBS). Brains were extracted from the skull, soaked in the fixative solution for 2 h, and cryoprotected in 30% sucrose phosphate buffer for 48 h. Brains were then frozen on dry ice, mounted onto a cryostat (Leica), and cut into serial coronal sections (80 μm-thick) that were immersed in PBS using multi-well dishes. The wet sections were temporarily mounted on glass slides for a preliminary microscopic visualization of TMR-dextran fluorescence (excitation—551 nm; emission—624 nm; Leica). Sections containing the injection site were examined first to verify successful labeling of a target cell body and its dendrites. If so, additional sections were mounted and inspected for the presence of axonal branches anywhere in the cortex, and, if so, all sections (about 175/brain) were immersed back in PBS and immunostained (see below) for brightfield microscopy (Leica).

Immunohistochemistry

Free-floating sections were incubated on a rotating platform in the following sequence: (*a*) pretreatment with 3:1 methanol/PBS solution containing 1% H_2O_2 to quench endogenous peroxidase activity (80 min, room temperature); (*b*) pre-incubation with PBS solution containing 2% fetal bovine serum albumin and 1% Triton X-100 to block nonspecific binding of the primary antibody (1 h, room temperature); (*c*) incubation with the primary antibody—rabbit anti-TMR (A-6397, Invitrogen)—diluted 1:3,000 in the pre-incubation solution (48 h, 4°C); (*d*) incubation with the secondary antibody—biotinylated goat anti-rabbit (Jackson ImmunoResearch Labs) diluted 1:500 in PBS (2 h, room temperature); (*e*) signal amplification and detection using avidin-biotin complex (ABC, Vector Labs) and nickel-enhanced staining with 3,3'-Diaminobenzidine (DAB). Sections were washed 3 times in 0.1 M PBS between each of the above steps. Consecutive immunostained sections were then mounted in order on glass slides and coverslipped with Cytoseal.

Mapping axonal projections

The cell body and processes of each labeled neuron were traced and reconstructed in aggregate using brightfield microscopy (200× magnification) and camera lucida technique (Olympus). Reconstruction started with sections containing labeled cell body and its dendritic tree, and continued from one section to the next along the trajectory of the parent axon and its subcortical and cortical termination fields, defined as collateral branches that bifurcated from the parent axon. Digital images of the cell body, dendrites, and axonal termination fields were also documented using scanning microscopy compiled from 1–1.5-μm-thick scans (Leica, LAS z-stacking software).

For detailed histological analysis of neuroanatomical structures and cortical lamination, the mounted sections were stripped from the coverslips, counterstained with neutral red and coverslipped again with Cytoseal. Digital images captured with scanning microscopy were used to mark the precise localization of the cell bodies of the labeled neurons and identify the cortical areas and laminae at their termination fields. Anatomical analysis was based on an atlas and a textbook of the rat brain (Vogt and Peters, 1981; Paxinos and Watson, 1998; DeFelipe et al., 2002; Shipp, 2007; Groh et al., 2010; Meyer et al., 2010).

Results

Using a glass micropipette preloaded with the anterograde tracer TMR-dextran, we isolated dura-sensitive and dura-insensitive neurons in several thalamic nuclei, and attempted to inject the tracer juxtacellularly into each of the target cell bodies (one neuron/rat). Of 53 such attempts, 17 cases were included in the analysis, as they resulted in successful singular labeling of the target cell body and its axonal terminal arbors in the cortex. Two additional cases of successful labeling were excluded from the analysis, as they resulted the in labeling

of two adjacent cell bodies, with no ability to determine which cell body and processes belonged to the target neuron. Of the remaining 34 attempts, 20 failed to produce any neuronal labeling, 9 yielded labeling of cell body but no processes, and 5 resulted in labeling of the cell body and the proximal part of the parent axon without detectable labeling in the cortex.

Neuronal classification, localization and morphology

Of the 17 labeled neurons included in the analysis, 12 were identified as dura-sensitive (Fig. 1A; Fig. 2A, red stars), 5 as dura-insensitive (Fig. 2A, blue stars).

Based on their responses to innocuous and noxious skin stimuli, the dura-sensitive group included wide-dynamic range (WDR) units (4 VPM, 1 Po); high-threshold (HT) units (3 Po, 2 LD, 1 LP); an unclassified Po unit that exhibited no excitatory cutaneous receptive field.

The dura-insensitive group included a WDR VPM neuron; a low-threshold (LT) VPM neuron that responded to deflections of a single vibrissae; a LT VPM neuron responsive to ophthalmic skin brushing; a Po neuron whose activity was inhibited by noxious stimulation of facial or body skin; an unclassified VPM neuron that exhibited no excitatory cutaneous receptive field.

The data below are dissected by neuronal identification (dura-sensitive vs. dura-insensitive units), and by the thalamic localization of the cell bodies (VPM, Po and LD/LP). Analysis by classification (nociceptive *vs.* non-nociceptive) was not feasible, as only two neurons were non-nociceptive (LT).

Cell-body size was similar between dura-sensitive and dura-insensitive units, and did not vary among the VPM, Po or LD/LP nuclei. The maximal dendritic spread (Fig. 2B) was also similar between dura-sensitive and dura-insensitive neurons. However, the dendritic tree of VPM neurons (263 ± 12 μm) was significantly smaller as compared to Po (352 ± 16) and LD/LP (344 ± 32) neurons ($p = 0.0054$, Kruskal-Wallis test).

Axonal trajectories from the thalamus to the cortex

The cell bodies sampled in this study were located between 3.3 and 4.4 mm caudal to the plane of the Bregma (Fig. 2). The parent axons typically projected forward, laterally and upward en route to the external capsule (Fig. 3), issuing prominent collateral arbors in the reticular (Rt) thalamic nucleus (Fig. 4). To identify the spatial organization of the subcortical axonal trajectories we analyzed the relative positions of the cell body and axonal entry points in the Rt and external capsule. Linear regression analyses of ten reconstructed neurons showed that the Rt arbor coordinates were correlated with the cell body position at the AP ($R^2 = 0.72$, $p = 0.0020$) and vertical ($R^2 = 0.66$, $p = 0.0044$) axes. The axonal entry points in the external capsule were, in turn, tightly correlated with the Rt arbor coordinates (AP: $R^2 = 0.75$, $p = 0.0013$; vertical: $R^2 = 0.77$, $p = 0.0009$; lateral: $R^2 = 0.73$, $p = 0.0016$). Additional collateral arbors were issued in the caudate putamen (CPu) by 4 of the 17 neurons (Fig. 5). Of those, 3 were dura-sensitive VPM units classified as WDR; one was a dura-insensitive Po neuron whose activity was inhibited by noxious skin stimulation.

Cortical projections of dura-sensitive neurons

VPM neurons (n = 4)—Dura-sensitive VPM neurons issued dense terminal arbors, which bifurcated from 1 or 2 branches of the parent axon, to the trigeminal barrel-field region of the primary somatosensory cortex (S1BF) and/or the secondary somatosensory cortex (S2). In addition, 2 of those neurons issued sparse collaterals in insular cortex, and a third neuron projected moderately into extra-trigeminal regions S1, and sparsely into the primary and

secondary motor cortices (M1/M2). Reconstruction of the cortical projections of one neuron is illustrated in Fig. 6A

Po neurons (n = 5)—Dura-sensitive Po neurons issued dense terminal arbors, which bifurcated from 1 or 2 branches of the parent axon, to S1BF and/or S2, as observed with their VPM counterparts. The Po units, however, also issued moderate-to-heavy projections to extra-trigeminal regions of S1, and to the primary auditory (AuD/Au1), retrosplenial (RSA), parietal association (PtA) and primary and secondary visual (V1/V2) cortices. One neuron projected heavily to the primary and secondary motor cortices (M1/M2) as well. Reconstructions of the cortical projections of two neurons are illustrated in Fig. 6B.

LD/LP neurons (n = 3)—One dura-sensitive LD neuron projected exclusively and heavily to M1/M2 (Fig. 7A). A second LD neuron projected lightly to M1/M2 and heavily to trigeminal and extratrigeminal regions of S1. The one LP neuron in this category exhibited dense terminal arbors in V2, sparse fibers in V1, and moderate arbors in the ectorhinal cortex (Fig. 7B).

Cortical projections of dura-insensitive neurons

Like dura-sensitive cells, all dura-insensitive neurons, regardless of their somatosensory classification (two LT, two HT, one unclassified) issued terminal arbors in S1BF and/or S2. The one dura-insensitive neuron that issued additional terminals in auditory and PtA cortices was nociceptive. Fig. 8 shows terminal arbors that arise from two LT dura-insensitive neurons in VPM (*A, B*) and one Po neuron whose activity was inhibited by noxious skin stimuli (*C*).

Cortical layers of termination

Somatosensory cortices—Terminal arbors were found in all layers of S1 and S2, with highest density in layers III and IV (Figs. 9–11). This general pattern was unrelated to thalamic localization of the cell body, dura sensitivity, or somatosensory classification.

Insular cortex—Layers III–VI of the insular cortex contained sparse-to-moderate density of labeled fibers arising from two dura-sensitive VPM neurons (Figs. 9, 12*A*) layers I–V were sparsely-to-moderately labeled by fibers arising from one dura-insensitive Po neuron (Fig. 9).

Parietal association cortex—Terminal fields in the PtA varied in density and layering patterns from neuron to neuron (Fig. 9): among three dura-sensitive Po neurons, one terminated sparsely in layers II and III (Fig. 12); a second terminated at various densities across layers I–V (most heavily in layers III–V); a third neuron projected lightly-to-moderately to layers II and III, and heavily to layer V. One dura-insensitive VPM neuron projected to all six layers of the PtA, most heavily to layers IV and V.

Retrosplenial cortex—In the RSA, layers I–III showed sparse-to-moderate density of fibers arising from four dura-sensitive Po neurons, with one of those neurons terminating densely in layer IV as well (Fig. 9).

Auditory and ectorhinal cortices—The AuD/Au1 cortices contained sparse labeling in layers II and III (Fig. 12*B*). In the ectorhinal cortex, most dense labeling was observed in layers V and VI (Fig. 12*C*). Layer I was devoid of labeled fibers in both the auditory and ectorhinal cortices (Fig. 9).

M1/M2—Sparse projections to layers V and VI arose from a dura-sensitive VPM unit; moderate-to-heavy projections to layers II and III from a dura-sensitive Po unit; and light or heavy projections to layers I–III from two dura-sensitive LD units (Figs. 9, 12*D*).

Visual cortex—Labeling in the visual cortex was only observed with dura-sensitive neurons (Figs. 9, 13). Terminal arbors of moderate-to-high density were observed in all layers of V1 and V2 overall, but the lamination pattern varied greatly from one neuron to the next (Fig. 9).

Discussion

This study unveiled the final thalamocortical limb of a pain pathway that is thought to underlie migraine headache. Most significant was the finding that each trigeminovascular neuron sampled in higher-order relay thalamic nuclei (Po, LD, LP) projected in multiple directions into anatomically-distinct cortical areas involved in functions as diverse as regulation of affect, motor capacity, visual and auditory perception, spatial orientation, memory retrieval, and olfaction. Furthermore, trigeminovascular neurons of the Po (a higher-order relay nucleus) projected well beyond the so-called “pain matrix” areas (S1, S2, insula), which were the main, if not exclusive, termination territory of their counterpart neurons in VPM (a first-order relay nucleus). This diverse pattern of connections arising from a single axon suggests that trigeminovascular neurons of higher-order relay thalamic nuclei are wired-ready to disseminate information to many cortical areas simultaneously and directly, which stands to explain the diversity of neurological disturbances associated with migraine headache. This pattern of direct projections to multiple cortices is distinct from the indirect, back-and-forth thalamocorticothalamic crosstalk which is mediated specifically by pyramidal cells in layer 5 of various cortical areas (Sherman, 2005; Jones, 2009).

Since the discussion of the extent of thalamocortical projections from each of the studied thalamic nuclei was based on a relatively small number of neurons, we cannot rule out the possibility that other neurons in the studied nuclei project to cortical areas not described here.

Dura-sensitive neurons have been identified previously in the thalamic VPM, Po and LP/LD nuclei (Davis and Dostrovsky, 1988b; Zagami and Lambert, 1990; Angus-Leppan et al., 1995; Shields and Goadsby, 2005; Burstein et al., 2010; Noseda et al., 2010). Based on the current study, we propose that dura-sensitive neurons in VPM, Po and LP/LD are capable of mediating different aspects of migraine headache, and that their different roles are determined by their distinct pattern of projections in the cortex (Fig. 14). For example, first-order relay dura-sensitive neurons in VPM project mainly to components of the so-called “pain matrix” (trigeminal S1, S2 and the insular cortex) and thus, are more likely to play a role in the perception of the headache (i.e., location, intensity and quality); whereas dense projections of individual higher-order relay dura-sensitive neurons in Po to non-trigeminal areas of S1, as well as auditory, visual, retrosplenial, ectorhinal and parietal association cortices may place them in a position to contribute more significantly to other aspects of the `migraine experience' which include disturbances in neurological functions involved in vision, auditory, memory, motor and cognitive performance and perhaps extended allodynia. In the context of thalamocorticothalamic processing, such interconnectivity may be considered as running in parallel to the well-defined “zig-zag” like circuit in which higher-order neurons relay sensory information from one cortical area to another through pyramidal cells in cortical layer 5 (Sherman, 2005; Jones, 2009).

Heavy projections of dura-sensitive neurons in all studied thalamic nuclei to the trigeminal area of S1, which follows the principles of thalamocortical projections of sensory thalamic

neurons (Meyer et al., 2010), suggest that they can also constitute a redundant network which ensures that critical information will be relayed from the thalamus to S1 and S2 in spite of the extensive modulation they are subjected to by neurons in layer 6 of the cortex and the reticular thalamic nucleus (Sherman, 2005; Jones, 2009).

Subcortical axonal trajectories of dura-sensitive VPM neurons differ from those of their counterparts in Po and LP/LD as they were the only one to issue terminal arborization in the basal ganglia. Although we have no functional explanation for this selectivity, the findings may explain the altered processing seen in this area during migraine (Afridi et al., 2005) and cluster headache (May et al., 2000).

Based on imaging studies of somatic pain (Coghill et al., 1994; Becerra et al., 1999; Tolle et al., 1999; Peyron et al., 2000; Bingel et al., 2003), we propose that the ability of migraineurs to perceive the source, severity and characteristics of headache involve nociceptive signals that reach the trigeminal area of S1, S2 and insula. S2 and the posterior insula have been implicated in encoding thermal pain intensity (Peyron et al., 1999; Zhang et al., 1999), which is manifested as thermal allodynia during migraine (Burstein et al., 2000). Moreover, evidence for amplification of activity in the thalamus, S2 and the posterior insular cortex following the provocation of pain by innocuous stimulation of the skin (Peyron et al., 1998) are in agreement with our proposal that sensitization of trigeminovascular thalamic neurons projecting to S2 and insula promotes extended allodynia during migraine (Burstein et al., 2010).

The anterior insula has been considered critical for normal processing of pain affect (Phillips et al., 1997; Buchel et al., 1999), and its lesion produced pain asymbolia, a condition in which individuals exhibit proper pain sensation but inappropriate pain affect (Berthier et al., 1988). This concept has been challenged recently in a study in which individuals with lesions of the insula (Starr et al., 2009) exhibited higher pain intensity rating and elevated pain-related activation of the primary somatosensory cortex; raising the possibility that the insula uses previously-acquired cognitive information to modulate the activity of other cortical areas that constitute the “pain-matrix” (Treede et al., 2000). In the context of migraine, projections of dura-sensitive thalamic neurons to the anterior insula, if present in humans, may play a role in fine-tuning incoming pain signals into other cortical areas involved in pain processing (i.e., S1, S2, prefrontal, anterior cingulate, amygdala, parahippocampal gyrus) by using cognitive information gained through previous experience with this recurrent pain disorder.

Another group of cortical areas that receive direct input from thalamic dura-sensitive neurons are members of a network of brain regions that support a range of cognitive functions which include spatial memory, navigation in space, imagination and planning for the future (Torrealba and Valdes, 2008; Vann et al., 2009). Of particular interest was the dense labeling in the PtA and RSA. The rat PtA (analogues to Brodmann areas 5 and 7) is thought to be involved in tasks that require association between different sensory modalities (Torrealba and Valdes, 2008). Functionally, the PtA is thought to play a role in determining where objects are in relation to parts of the body which is critical for proper ability to locate objects in space. In the context of migraine, input to this areas from dura-sensitive neurons may explain what appears to patients as motor clumsiness and difficulty in focusing attention on particular tasks in a complex environment with multiple distractions. The RSA (analogues to Brodmann areas 29 and 30) is considered essential for acquiring new information, retrieval of short-term autobiographical events, successful navigation through familiar environment, and speech production and comprehension (Vann et al., 2009); (Valenstein et al., 1987; Maguire, 2001; Awad et al., 2007). In the context of migraine, input

to the RSA from dura-sensitive neurons, if exists in the human, may contribute to the transient decline in speech production and comprehension, as well as cognitive functions.

Under normal conditions, the motor cortex exhibits 20-Hz oscillatory activity which is essential for setting up proper level of intracortical inhibition and inhibition of thalamic relay neurons (Peyron et al., 1995; Garcia-Larrea et al., 1999). Since this oscillatory activity is disrupted in the presence of chronic or evoked pain (Juottonen et al., 2002; Raij et al., 2004; Lefaucheur, 2006), it is tempting to propose that projections of dura-sensitive thalamic neurons to the primary motor cortex may promote cortical hyperexcitability in migraineurs. Critical to future understanding of migraine pathophysiology is whether attack frequency and associated symptoms are results of inherent defect in motor cortex ability to govern cortical excitability and activity of descending modulatory pain pathways in the brainstem, or a breakdown of oscillatory activity following repeated bombardment of its neurons by the noxious inputs it receives during migraine.

Given our recent description of direct retino-thalamo-cortical pathway for exacerbation of migraine by light (Noseda et al., 2010), it may not be surprising that dura-sensitive neurons in higher-order relay nuclei project heavily to all layers of the visual (as well as other) cortices. Although speculative, enhanced firing in these neurons due to nociceptive input from the dura may interfere with proper cortical processing of photic signals. In the context of migraine, such disruption may mediate the perception of blurred or double vision, saturation of colors and the abnormal intolerance to light (Liveing, 1873). Similarly, projections of these dura-sensitive neurons to the auditory cortices may alter proper cortical processing of auditory signals, resulting in extreme intolerance to noise.

In agreement with the literature (Shipp, 2007; Wimmer et al., 2010), dura-sensitive neurons in VPM and Po issued terminal arborization in all cortical layers of the somatosensory and visual cortices and in almost all layers of the other cortical areas they project to. The absence of terminal arborization in layer 6 of the RSA, PtA and the motor cortex may be significant in migraine pathophysiology if holds true in future studies of a much greater scale. Given the input to all layers, it seems reasonable to propose that activation of dura-sensitive thalamic neurons during migraine can set off localized and intrahemispheric communication needed for modulation of pyramidal cells in layers 5 and 6 which respectively regulate cranial nerves and sensory and motor spinal cord neurons, and most importantly the thalamic input to the cortex.

We cannot conclude with certainty that the widespread thalamocortical projections are unique to dura-sensitive neurons. However, in view of the limited cortical projections of nociceptive thalamic neurons that respond to somatic skin stimulation (Gauriau and Bernard, 2004; Monconduit and Villanueva, 2005; Monconduit et al., 2006), we suggest that the projection pattern of dura-sensitive neurons may be a distinct feature of the trigeminovascular pathway.

Acknowledgments

This research was supported by NIH grants NS-051484 and NS-069847 (RB).

References

Afridi SK, Matharu MS, Lee L, Kaube H, Friston KJ, Frackowiak RS, Goadsby PJ. A PET study exploring the laterality of brainstem activation in migraine using glyceryl trinitrate. Brain. 2005

Angus-Leppan H, Lambert GA, Michalicek J. Convergence of occipital nerve and superior sagittal sinus input in the cervical spinal cord of the cat. Cephalalgia. 1997; 17:625–630. discussion 623. [PubMed: 9350381]

Angus-Leppan H, Olausson B, Boers P, Lambert GA. Convergence of afferents from superior sagittal sinus and tooth pulp on cells in the thalamus of the cat. Cephalalgia. 1995; 15:191–199. [PubMed: 7553808]

Awad M, Warren JE, Scott SK, Turkheimer FE, Wise RJ. A common system for the comprehension and production of narrative speech. J Neurosci. 2007; 27:11455–11464. [PubMed: 17959788]

Becerra LR, Breiter HC, Stojanovic M, Fishman S, Edwards A, Comite AR, Gonzalez RG, Borsook D. Human brain activation under controlled thermal stimulation and habituation to noxious heat: an fMRI study. Magn Reson Med. 1999; 41:1044–1057. [PubMed: 10332889]

Berthier M, Starkstein S, Leiguarda R. Asymbolia for pain: a sensory-limbic disconnection syndrome. Ann Neurol. 1988; 24:41–49. [PubMed: 3415199]

Bingel U, Quante M, Knab R, Bromm B, Weiller C, Buchel C. Single trial fMRI reveals significant contralateral bias in responses to laser pain within thalamus and somatosensory cortices. NeuroImage. 2003; 18:740–748. [PubMed: 12667851]

Buchel C, Dolan RJ, Armony JL, Friston KJ. Amygdala-hippocampal involvement in human aversive trace conditioning revealed through event-related functional magnetic resonance imaging. J Neurosci. 1999; 19:10869–10876. [PubMed: 10594068]

Burstein R, Yamamura H, Malick A, Strassman AM. Chemical stimulation of the intracranial dura induces enhanced responses to facial stimulation in brain stem trigeminal neurons. Journal of Neurophysiology. 1998; 79:964–982. [PubMed: 9463456]

Burstein R, Yarnitsky D, Goor-Aryeh I, Ransil BJ, Bajwa ZH. An association between migraine and cutaneous allodynia. Annals Neurol. 2000; 47:614–624.

Burstein R, Jakubowski M, Garcia-Nicas E, Kainz V, Bajwa Z, Hargreaves R, Becerra L, Borsook D. Thalamic sensitization transforms localized pain into widespread allodynia. Ann Neurol. 2010; 68:81–91. [PubMed: 20582997]

Coghill RC, Talbot JD, Evans AC, Meyer E, Gjedde A, Bushnell MC, Duncan GH. Distributed processing of pain and vibration by the human brain. Journal of Neuroscience. 1994; 14:4095–4108. [PubMed: 8027764]

Davis KD, Dostrovsky JO. Responses of feline trigeminal spinal tract nucleus neurons to stimulation of the middle meningeal artery and sagittal sinus. Journal of Neurophysiology. 1988a; 59:648–666. [PubMed: 3351579]

Davis KD, Dostrovsky JO. Properties of feline thalamic neurons activated by stimulation of the middle meningeal artery and sagittal sinus. Brain research. 1988b; 454:89–100. [PubMed: 3409027]

DeFelipe J, Alonso-Nanclares L, Arellano JI. Microstructure of the neocortex: comparative aspects. J Neurocytol. 2002; 31:299–316. [PubMed: 12815249]

Ebersberger A, Ringkamp M, Reeh PW, Handwerker HO. Recordings from brain stem neurons responding to chemical stimulation of the subarachnoid space. Journal of Neurophysiology. 1997; 77:3122–3133. [PubMed: 9212262]

Garcia-Larrea L, Peyron R, Mertens P, Gregoire MC, Lavenne F, Le Bars D, Convers P, Mauguiere F, Sindou M, Laurent B. Electrical stimulation of motor cortex for pain control: a combined PET-scan and electrophysiological study. Pain. 1999; 83:259–273. [PubMed: 10534598]

Gauriau C, Bernard JF. Posterior triangular thalamic neurons convey nociceptive messages to the secondary somatosensory and insular cortices in the rat. J Neurosci. 2004; 24:752–761. [PubMed: 14736861]

Groh A, Meyer HS, Schmidt EF, Heintz N, Sakmann B, Krieger P. Cell-type specific properties of pyramidal neurons in neocortex underlying a layout that is modifiable depending on the cortical area. Cereb Cortex. 2010; 20:826–836. [PubMed: 19643810]

Jones EG. Synchrony in the interconnected circuitry of the thalamus and cerebral cortex. Ann N Y Acad Sci. 2009; 1157:10–23. [PubMed: 19351352]

Juottonen K, Gockel M, Silen T, Hurri H, Hari R, Forss N. Altered central sensorimotor processing in patients with complex regional pain syndrome. Pain. 2002; 98:315–323. [PubMed: 12127033]

Kaube H, Hoskin KL, Goadsby PJ. Activation of the trigeminovascular system by mechanical distension of the superior sagittal sinus in the cat [see comments]. Cephalalgia. 1992; 12:133–136. [PubMed: 1623506]

Lefaucheur JP. The use of repetitive transcranial magnetic stimulation (rTMS) in chronic neuropathic pain. Neurophysiol Clin. 2006; 36:117–124. [PubMed: 17046606]

Levy D, Strassman AM. Mechanical response properties of A and C primary afferent neurons innervating the rat intracranial dura. Journal of Neurophysiology. 2002; 88:3021–3031. [PubMed: 12466427]

Liu Y, Broman J, Edvinsson L. Central projections of sensory innervation of the rat superior sagittal sinus. Neuroscience. 2004; 129:431–437. [PubMed: 15501600]

Liu Y, Broman J, Edvinsson L. Central projections of the sensory innervation of the rat middle meningeal artery. Brain Res. 2008; 1208:103–110. [PubMed: 18395192]

Liveing, E. On megrim, sick headache. Arts & Boeve Publishers; Nijmegen: 1873.

Maguire EA. The retrosplenial contribution to human navigation: a review of lesion and neuroimaging findings. Scand J Psychol. 2001; 42:225–238. [PubMed: 11501737]

May A, Bahra A, Buchel C, Frackowiak RS, Goadsby PJ. PET and MRA findings in cluster headache and MRA in experimental pain. Neurology. 2000; 55:1328–1335. [PubMed: 11087776]

Mayberg M, Langer RS, Zervas NT, Moskowitz MA. Perivascular meningeal projections from cat trigeminal ganglia: possible pathway for vascular headaches in man. Science (New York, NY. 1981; 213:228–230.

Mayberg MR, Zervas NT, Moskowitz MA. Trigeminal projections to supratentorial pial and dural blood vessels in cats demonstrated by horseradish peroxidase histochemistry. Journal of Comparative Neurology. 1984; 223:46–56. [PubMed: 6200513]

Meyer HS, Wimmer VC, Hemberger M, Bruno RM, de Kock CP, Frick A, Sakmann B, Helmstaedter M. Cell type-specific thalamic innervation in a column of rat vibrissal cortex. Cereb Cortex. 2010; 20:2287–2303. [PubMed: 20534783]

Monconduit L, Villanueva L. The lateral ventromedial thalamic nucleus spreads nociceptive signals from the whole body surface to layer I of the frontal cortex. Eur J Neurosci. 2005; 21:3395–3402. [PubMed: 16026477]

Monconduit L, Lopez-Avila A, Molat JL, Chalus M, Villanueva L. Corticofugal output from the primary somatosensory cortex selectively modulates innocuous and noxious inputs in the rat spinothalamic system. Journal of Neuroscience. 2006; 26:8441–8450. [PubMed: 16914669]

Noseda R, Kainz V, Jakubowski M, Gooley JJ, Saper CB, Digre K, Burstein R. A neural mechanism for exacerbation of headache by light. Nat Neurosci. 2010; 13:239–245. [PubMed: 20062053]

Paxinos, G.; Watson, C. The Rat Brain in Stereotaxic Coordinates. Fourth Edition. Academic Press; Orlando: 1998.

Peyron R, Laurent B, Garcia-Larrea L. Functional imaging of brain responses to pain. A review and meta-analysis (2000). Neurophysiol Clin. 2000; 30:263–288. [PubMed: 11126640]

Peyron R, Garcia-Larrea L, Deiber MP, Cinotti L, Convers P, Sindou M, Mauguiere F, Laurent B. Electrical stimulation of precentral cortical area in the treatment of central pain: electrophysiological and PET study. Pain. 1995; 62:275–286. [PubMed: 8657427]

Peyron R, GarciaLarrea L, Gregoire MC, Costes N, Convers P, Lavenne F, Mauguiere F, Michel D, Laurent B. Haemodynamic brain responses to acute pain in humans - Sensory and attentional networks. Brain. 1999; 122:1765–1779. [PubMed: 10468515]

Peyron R, Garcia-Larrea L, Gregoire MC, Convers P, Lavenne F, Veyre L, Froment JC, Mauguiere F, Michel D, Laurent B. Allodynia after lateral-medullary (Wallenberg) infarct. A PET study. Brain. 1998; 121(Pt 2):345–356. [PubMed: 9549510]

Phillips ML, Young AW, Senior C, Brammer M, Andrew C, Calder AJ, Bullmore ET, Perrett DI, Rowland D, Williams SC, Gray JA, David AS. A specific neural substrate for perceiving facial expressions of disgust. Nature. 1997; 389:495–498. [PubMed: 9333238]

Raij TT, Forss N, Stancak A, Hari R. Modulation of motor-cortex oscillatory activity by painful Adelta- and C-fiber stimuli. NeuroImage. 2004; 23:569–573. [PubMed: 15488406]

Sherman SM. Thalamic relays and cortical functioning. Prog Brain Res. 2005; 149:107–126. [PubMed: 16226580]

Shields KG, Goadsby PJ. Propranolol modulates trigeminovascular responses in thalamic ventroposteromedial nucleus: a role in migraine? Brain. 2005; 128:86–97. [PubMed: 15574468]

Shipp S. Structure and function of the cerebral cortex. Curr Biol. 2007; 17:R443–449. [PubMed: 17580069]

Starr CJ, Sawaki L, Wittenberg GF, Burdette JH, Oshiro Y, Quevedo AS, Coghill RC. Roles of the insular cortex in the modulation of pain: insights from brain lesions. J Neurosci. 2009; 29:2684–2694. [PubMed: 19261863]

Strassman AM, Mineta Y, Vos BP. Distribution of fos-like immunoreactivity in the medullary and upper cervical dorsal horn produced by stimulation of dural blood vessels in the rat. J Neurosci. 1994; 14:3725–3735. [PubMed: 8207485]

Strassman AM, Raymond SA, Burstein R. Sensitization of meningeal sensory neurons and the origin of headaches. Nature. 1996; 384:560–564. [PubMed: 8955268]

Tolle TR, Kaufmann T, Siessmeier T, Lautenbacher S, Berthele A, Munz F, Zieglgansberger W, Willoch F, Schwaiger M, Conrad B, Bartenstein P. Region-specific encoding of sensory and affective components of pain in the human brain: a positron emission tomography correlation analysis. Ann Neurol. 1999; 45:40–47. [PubMed: 9894875]

Torrealba F, Valdes JL. The parietal association cortex of the rat. Biol Res. 2008; 41:369. [PubMed: 19621117]

Treede RD, Apkarian AV, Bromm B, Greenspan JD, Lenz FA. Cortical representation of pain: functional characterization of nociceptive areas near the lateral sulcus. Pain. 2000; 87:113–119. [PubMed: 10924804]

Valenstein E, Bowers D, Verfaellie M, Heilman KM, Day A, Watson RT. Retrosplenial amnesia. Brain. 1987; 110(Pt 6):1631–1646. [PubMed: 3427404]

Vann SD, Aggleton JP, Maguire EA. What does the retrosplenial cortex do? Nat Rev Neurosci. 2009; 10:792–802. [PubMed: 19812579]

Vogt BA, Peters A. Form and distribution of neurons in rat cingulate cortex: areas 32, 24, and 29. The Journal of comparative neurology. 1981; 195:603–625. [PubMed: 7462444]

Wimmer VC, Bruno RM, de Kock CP, Kuner T, Sakmann B. Dimensions of a projection column and architecture of VPM and POm axons in rat vibrissal cortex. Cereb Cortex. 2010; 20:2265–2276. [PubMed: 20453248]

Yamamura H, Malick A, Chamberlin NL, Burstein R. Cardiovascular and neuronal responses to head stimulation reflect central sensitization and cutaneous allodynia in a rat model of migraine. Journal of Neurophysiology. 1999; 81:479–493. [PubMed: 10036252]

Zagami AS, Lambert GA. Stimulation of cranial vessels excites nociceptive neurones in several thalamic nuclei of the cat. Experimental Brain Research. 1990; 81:552–566.

Zagami AS, Lambert GA. Craniovascular application of capsaicin activates nociceptive thalamic neurones in the cat. Neurosci Lett. 1991; 121:187–190. [PubMed: 1708477]

Zhang ZH, Dougherty PM, Oppenheimer SM. Monkey insular cortex neurons respond to baroreceptive and somatosensory convergent inputs. Neuroscience. 1999; 94:351–360. [PubMed: 10579199]

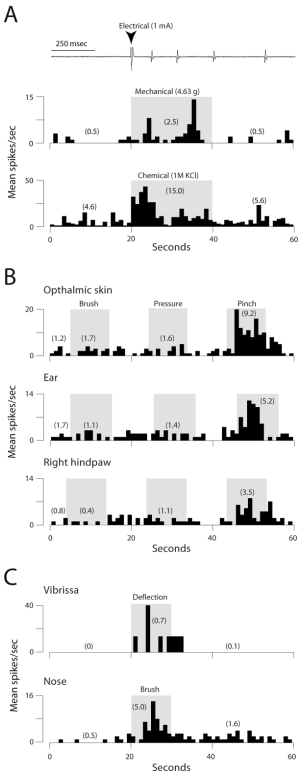

Figure 1.

Identification and classification of trigeminovascular thalamic neurons. ***A***, Individual dura-sensitive neurons exhibited discrete discharges in responses to electrical, mechanical, and chemical stimulation of the cranial dura overlying the transverse sinus. ***B***, Dura-sensitive neurons that responded to noxious stimulation of the skin (pinch) were classified as nociceptive if they exhibited no discharge in response to innocuous skin stimuli (brush, pressure). ***C***, Dura-sensitive neurons that responded to gentle mechanical stimulation were classified as non-nociceptive. Stimulus intervals are indicated by gray areas. Numbers in parentheses are spikes/sec for the corresponding intervals. Bin width = 1 sec.

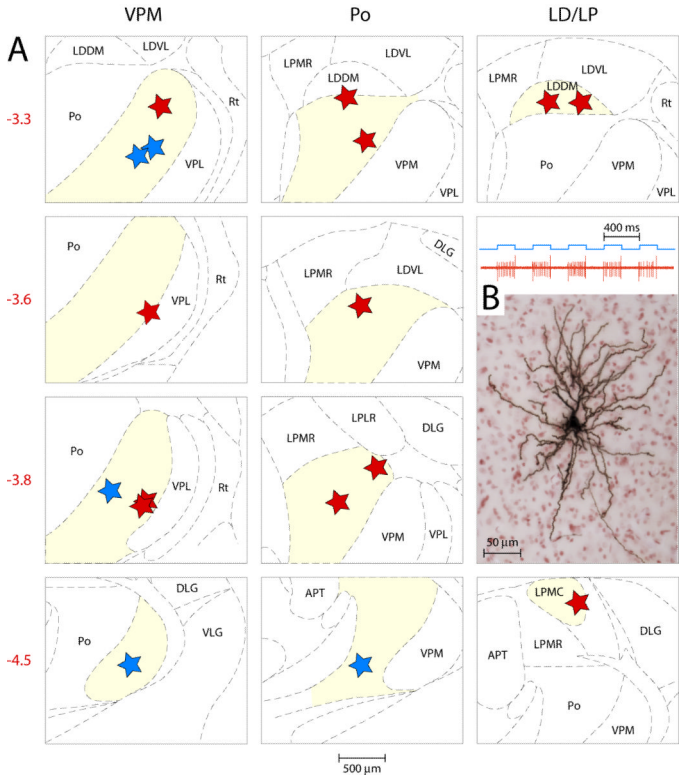

Figure 2.

Localization of dura-sensitive (red stars) and dura-insensitive (blue stars) neurons in the thalamus. ***A***, Localization of the cell bodies in the VPM, Po, and LD and LP nuclei (each nucleus highlighted in yellow). Numbers in red indicate the coronal plane (mm from Bregma) according to the rat brain atlas (Paxinos and Watson, 1998). ***B***, A photomicrograph of the cell body and dendritic tree of a dura-sensitive (LP) neuron that was labeled with the anterograde tracer TMR–dextran. Uptake of the tracer by the target cell body was achieved by inducing bouts of neuronal firing (red trace) in response to repetitive electrical pulses (blue trace) delivered from the recording micropipette, which was preloaded with the tracer. Abbreviations: APT, anterior pretectal nucleus; DLG, dorsal lateral geniculate nucleus; LDDM, laterodorsal thalamic nucleus, dorsomedial; LDVL, laterodorsal thalamic nucleus, ventrolateral; LPMR, lateral posterior thalamic nucleus, mediorostral; Po, posterior thalamic nuclear group; Rt, reticular thalamic nucleus; VPL, ventral posterolateral thalamic nucleus; VPM, ventral posteromedial thalamic nucleus.

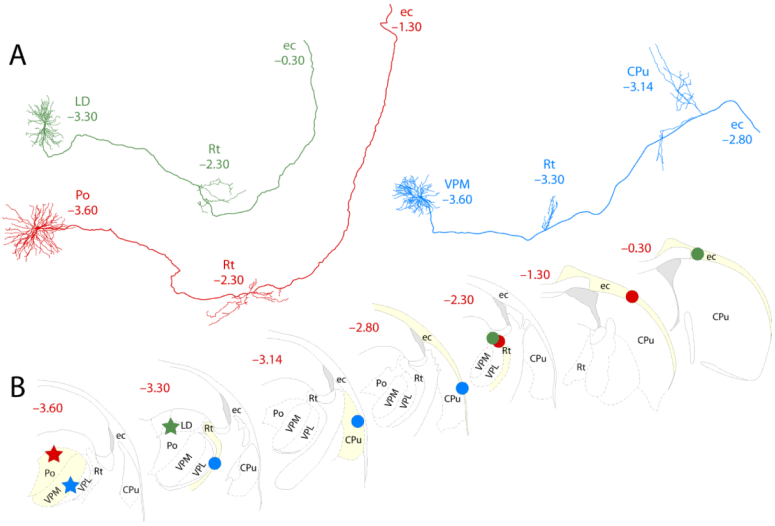

Figure 3.

Subcortical mapping of axonal projections and their collaterals. ***A***, Two-dimensional camera-lucida reconstruction of cell bodies and dendritic trees of three dura-sensitive thalamocortical neurons, their collateral arbors in the reticular thalamic nucleus (Rt) and caudate putamen (CPu), and their entry point in the external capsule (ec). ***B***, Localization of the cell bodies (stars) and landmarks of axonal trajectories (circles) of the neurons reconstructed above. Numbers in *A* and *B* indicate the coronal plane (mm from Bregma). Color coding is the same in **A** and **B**.

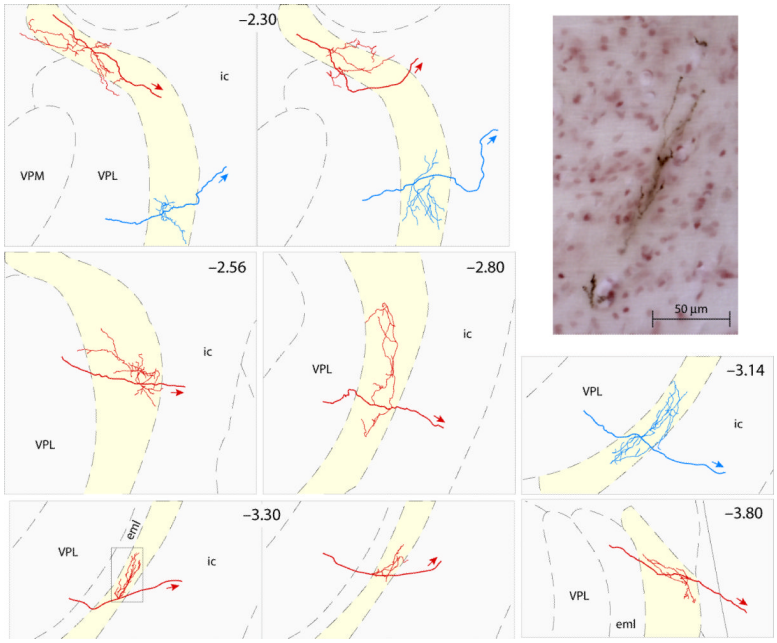

Figure 4.

Reconstruction of individual axonal arbors in the reticular thalamic nucleus. The parent axons and their trajectories are indicated by arrows. Dura-sensitive neurons are red. Dura-insensitive neurons are blue. The photomicrograph corresponds to the box in lower left panel. Numbers indicate the coronal plane (mm from Bregma). Abbreviations: eml, external medullary lamina; ic, internal capsule.

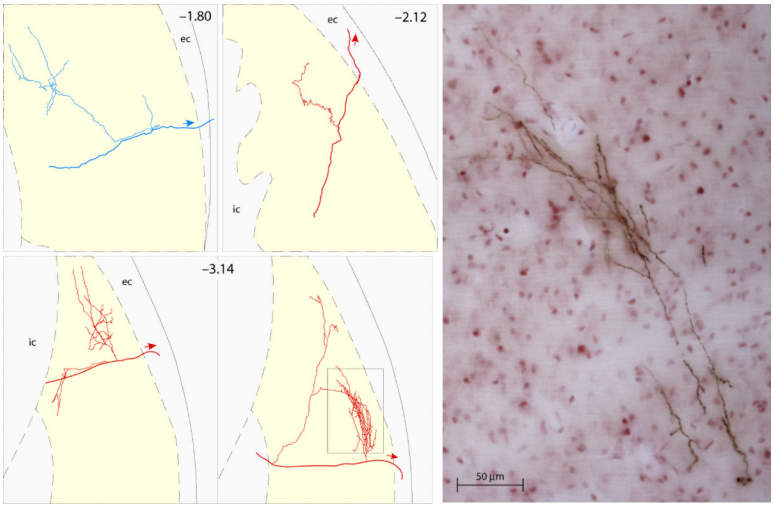

Figure 5.
Reconstruction of individual axonal arbors in the caudate putamen. The parent axons and their trajectories are indicated by arrows. Dura-sensitive neurons are red. Dura-insensitive neurons are blue. The photomicrograph corresponds to the box in lower right panel. Numbers indicate the coronal plane (mm from Bregma).

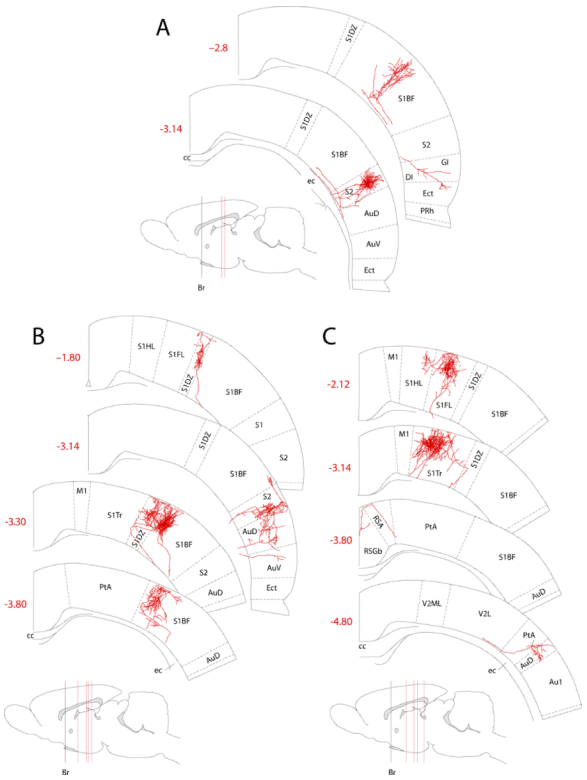

Figure 6.

Reconstruction of cortical axonal arbors of individual dura-sensitive VPM (*A*) and Po (**B, C**) neurons. Numbers in red indicate the coronal plane (mm from Bregma). The levels of the different coronal drawings are indicated as red lines in the sagittal drawing of the brain. Note that VPM neurons project mainly to S1, S2 and the insula whereas Po neurons project to multiple cortical areas outside the so-called “pain matrix”. Abbreviations: Au1, primary auditory cortex; AuD, secondary auditory cortex, dorsal; AuV, secondary auditory cortex, ventral; Br, Bregma; cc, corpus callosum; DI, dysgranular insular cortex; Ect, Ectorhinal cortex; GI, granular insular cortex; M1, primary motor cortex; PtA, parietal association cortex; PRh, perirhinal cortex; RSA, retrosplenial cortex; RSGb, retrosplenial granular cortex, b; S1, primary somatosensory cortex; S1BF, primary somatosensory cortex, barrel field; S1DZ, primary somatosensory cortex, dysgranular; S1FL, primary somatosensory cortex, forelimb; S1HL, primary somatosensory cortex, hindlimb; S1Tr, primary somatosensory cortex, trunk area; S2, secondary somatosensory cortex; V2L, secondary visual cortex, lateral area; V2ML, secondary visual cortex, mediolateral.

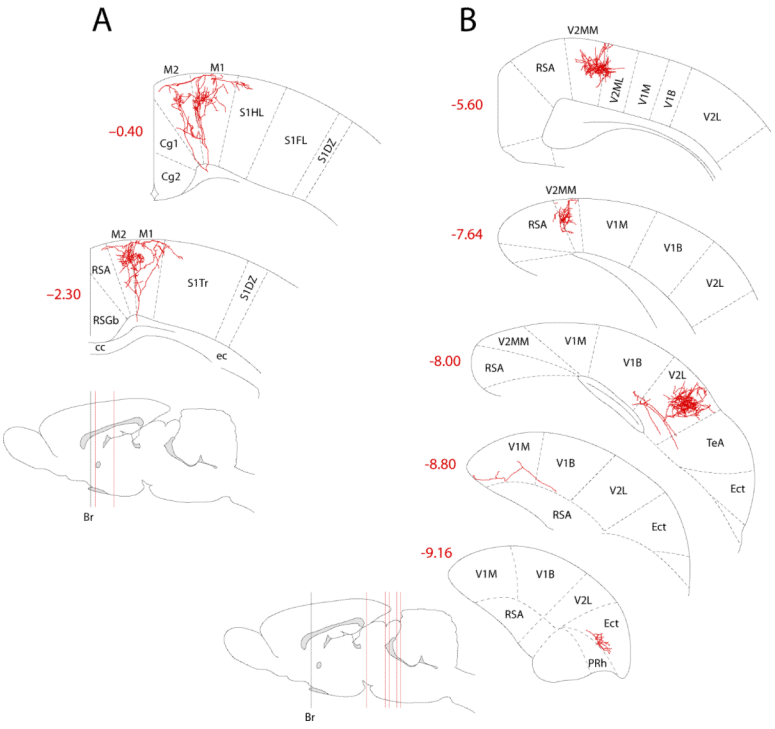

Figure 7.

Reconstruction of cortical axonal arbors of individual dura-sensitive LD (***A***) and LP (***B***) neurons. Note massive projections to visual and motor cortices. Abbreviations: Cg1, cingulated cortex, area 1; Cg2, cingulated cortex, area 2; M2, secondary motor cortex; V1B, primary visual cortex, binocular; V1M, primary visual cortex, monocular; V2MM, secondary visual cortex, mediomedial; TeA, temporal association cortex. See Fig. 6 for additional information and abbreviations.

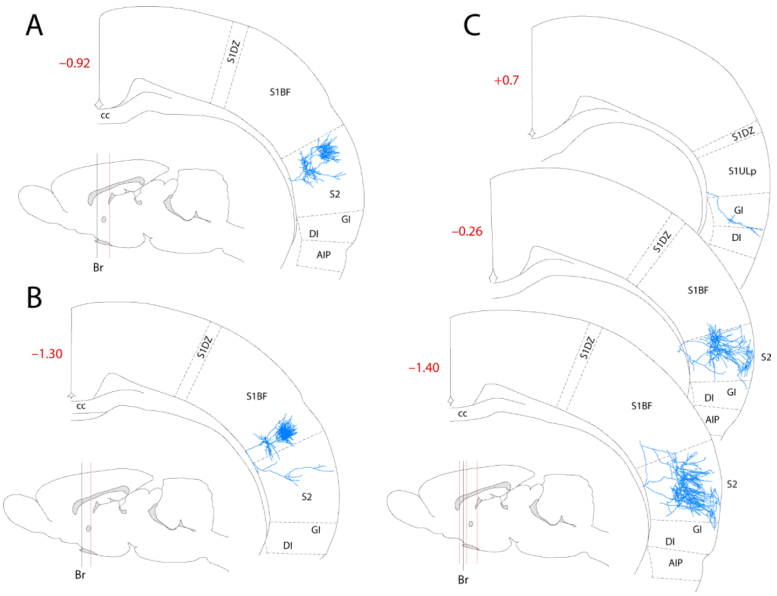

Figure 8.

Reconstruction of cortical axonal arbors of individual dura-insensitive VPM (***A, B***) and Po (***C***) neurons. Note that most terminal arborization was restricted to cortical areas that process somatosensory information. Abbreviations: AIP, agranular insular cortex, posterior; GIDI, S1Jo, S1ULp, primary somatosensory cortex, upper lip. See Fig. 6 for additional information.

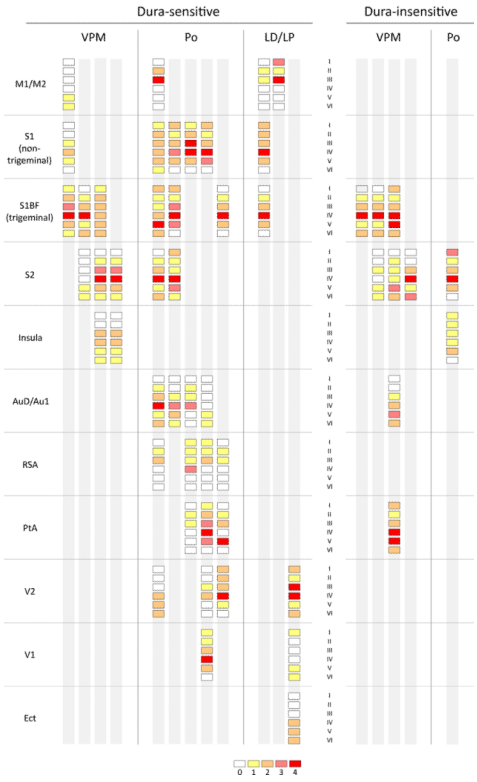

Figure 9.
Relative laminar density of terminal arbors of dura-sensitive and dura-insensitive thalamocortical neurons. Fiber density (0–4) is color-coded according to the scale at the bottom.

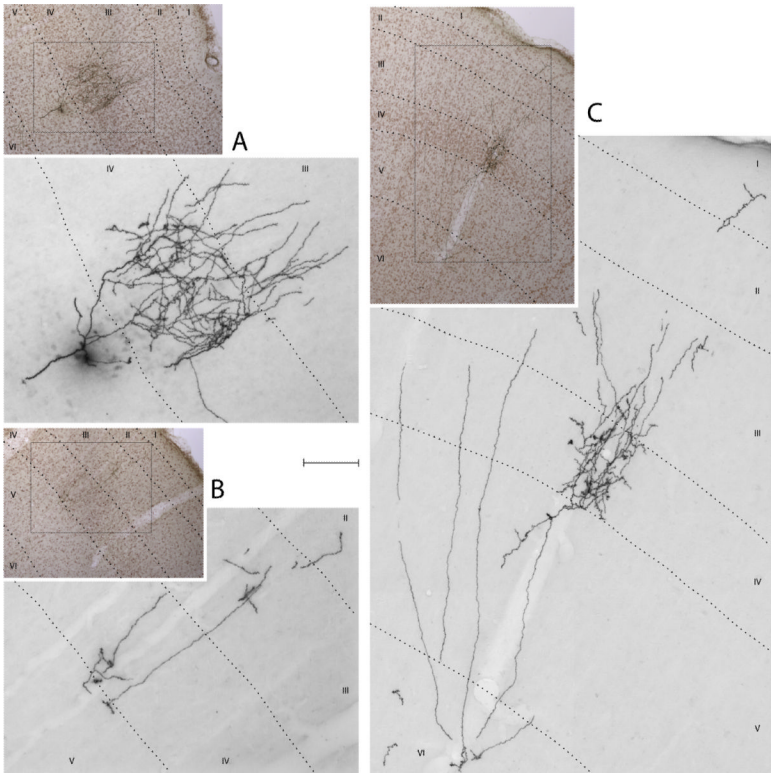

Figure 10.
Photomicrographs of axonal arbors in the trigeminal S1 area (S1BF). ***A***, Dura-insensitive VPM neuron. ***B, C***, Dura-sensitive VPM neurons. Roman numerals mark the cortical layers. Immunostained fibers were captured before (monochrome images) and after counterstaining of the tissue with neutral red (color images). Boxed areas in the color images correspond to the higher-power monochrome images. Scale bar = 300 and 100 μm for color and monochrome images, respectively.

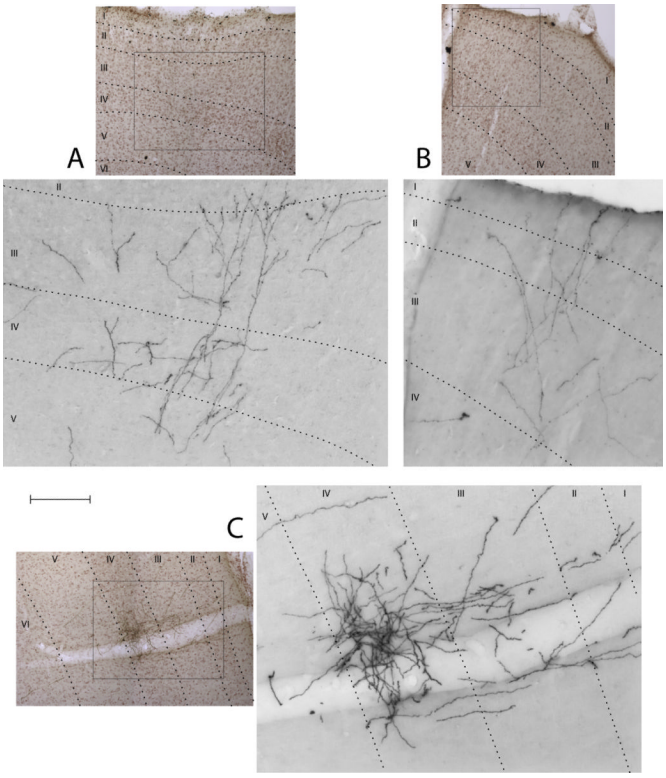

Figure 11.
Photomicrographs of axonal arbors in extratrigeminal S1 areas and S2. ***A***, S1Tr (trunk), dura-sensitive Po neuron. ***B***, S1HL (hindlimb), dura-sensitive Po neuron. ***C***, S2, dura-sensitive VPM neuron. See Fig. 10 for additional information, including cortical layers and scales.

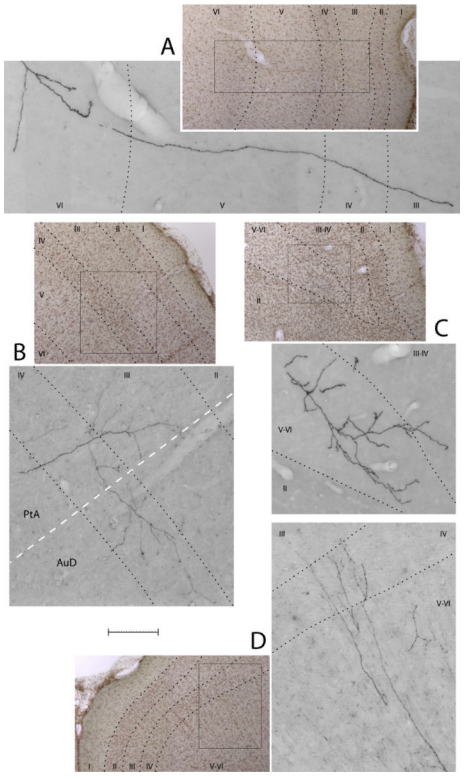

Figure 12.

Photomicrographs of axonal arbors in insular, auditory, parietal, ectorhinal and motor cortices. ***A***, Insula, dura-sensitive VPM neuron. ***B***, PtA and AuD, dura-sensitive Po neuron. ***C***, Ectorhinal, dura-sensitive LP neuron. ***D***, M1/M2, dura-sensitive LD neuron. See Fig. 10 for additional information, including cortical layers and scales.

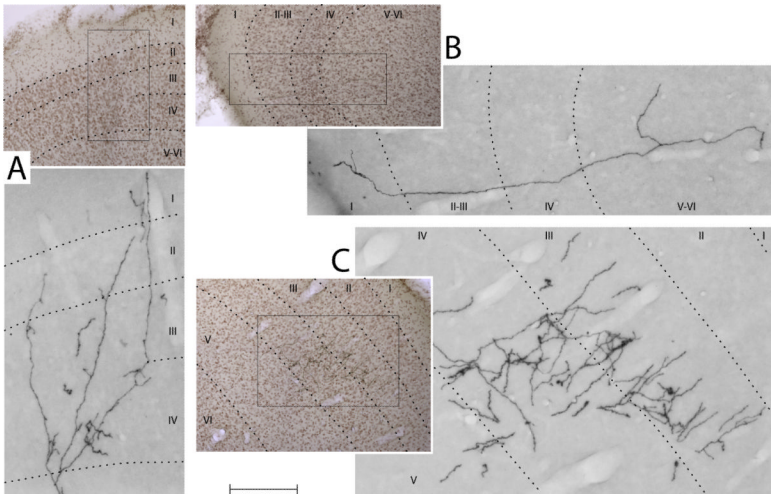

Figure 13.

Photomicrographs of axonal arbors in the visual cortices of a dura-sensitive LP neuron. ***A***, V2MM. ***B*** V1M. ***C***, V2L. See Fig. 10 for additional information, including cortical layers and scales.

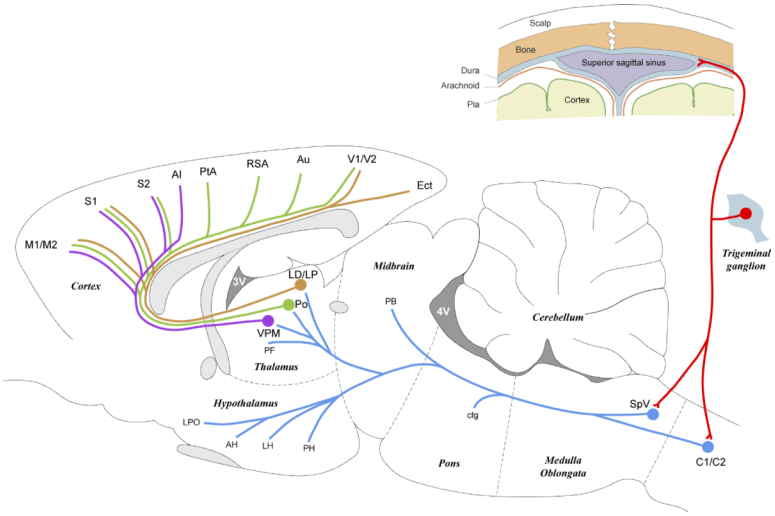

Figure 14.

Schematic illustration of the trigeminovascular pathway between the meninges and the cortex. The peripheral limb (meningeal nociceptors) is shown in red. The ascending limb from the spinal trigeminal nucleus (Vc and C1/C2) to the brainstem, thalamus and hypothalamus is shown in blue. The thalamocortical projections from VPM, PO and LD/LP are shown in purple, green and orange, respectively. Abbreviations:; AH, anterior hypothalamus; ctg, central tegmental area; LH, lateral hypothalamus; LPO, lateral posterior area; PB, parabrachial area; PH, posterior hypothalamus. For additional abbreviations see previous Fig. legends.